

Chemical-genomic dissection of the CTD code

Joshua R Tietjen¹, David W Zhang^{1,5}, Juan B Rodríguez-Molina^{1,5}, Brent E White^{1,5}, Md Sohail Akhtar¹, Martin Heidemann², Xin Li^{1,3}, Rob D Chapman², Kevan Shokat⁴, Sündüz Keles³, Dirk Eick² & Asem Z Ansari¹

Sequential modifications of the RNA polymerase II (Pol II) C-terminal domain (CTD) coordinate the stage-specific association and release of cellular machines during transcription. Here we examine the genome-wide distributions of the ‘early’ (phospho-Ser5 (Ser5-P)), ‘mid’ (Ser7-P) and ‘late’ (Ser2-P) CTD marks. We identify gene class-specific patterns and find widespread co-occurrence of the CTD marks. Contrary to its role in 3’-processing of noncoding RNA, the Ser7-P marks are placed early and retained until transcription termination at all Pol II-dependent genes. Chemical-genomic analysis reveals that the promoter-distal Ser7-P marks are not remnants of early phosphorylation but are placed anew by the CTD kinase Bur1. Consistent with the ability of Bur1 to facilitate transcription elongation and suppress cryptic transcription, high levels of Ser7-P are observed at highly transcribed genes. We propose that Ser7-P could facilitate elongation and suppress cryptic transcription.

The C-terminal domain (CTD) of the largest subunit of RNA polymerase II (Pol II) orchestrates dynamic interactions with proteins that are required for various stages of transcription¹. The structural plasticity of the CTD and its proximity to the RNA exit tunnel of the polymerase enable it to interact with multiple protein complexes, including those that process the nascent transcript (**Supplementary Fig. 1**). The CTD is composed of 26 repeating heptapeptides (Tyr1-Ser2-Pro3-Thr4-Ser5-Pro6-Ser7) in budding yeast. Five of the seven residues (Tyr1, Ser2, Thr4, Ser5 and Ser7) can be phosphorylated or glycosylated, and the proline residues (Pro3 and Pro6) can exist in two stereoisomeric states (*cis* or *trans*). The stage-specific association and exchange of protein partners is mediated by sequential post-translational modifications of different residues of the heptapeptide repeats^{1–4}. During transcription initiation, Ser5 residues of the CTD are phosphorylated by the Kin28/Cdk7 subunit of transcription factor IIH and by the Srb10/Cdk8 subunit of the Mediator complex^{5–10}. This ‘early’ modification releases Pol II from the promoter-bound preinitiation complex^{8,11} and facilitates the association of the capping enzyme complex and the Set1 histone methyltransferase^{12–16}. Shortly after promoter release, Rtr1, an atypical phosphatase, erases the phospho-Ser5 (Ser5-P) marks on the elongating Pol II¹⁷. Next, the Cdk9 kinase of the positive transcription elongation factor b complex phosphorylates the Ser2 residues of the CTD^{7,18}. This ‘late’ post-translational mark facilitates transcription elongation as well as the association of splicing factors and the Set2 histone methyltransferase that places repressive marks, thus preventing cryptic transcription within coding regions^{1,4,19,20}. In *Saccharomyces cerevisiae*, the role of Cdk9 is split between two homologous kinases, Ctk1 and Bur1 (ref. 21). Ctk1 is the primary Ser2 kinase, whereas Bur1 is thought to stimulate elongation and suppress cryptic transcription by acting on non-CTD substrates^{21–25}. Toward the end of the coding region,

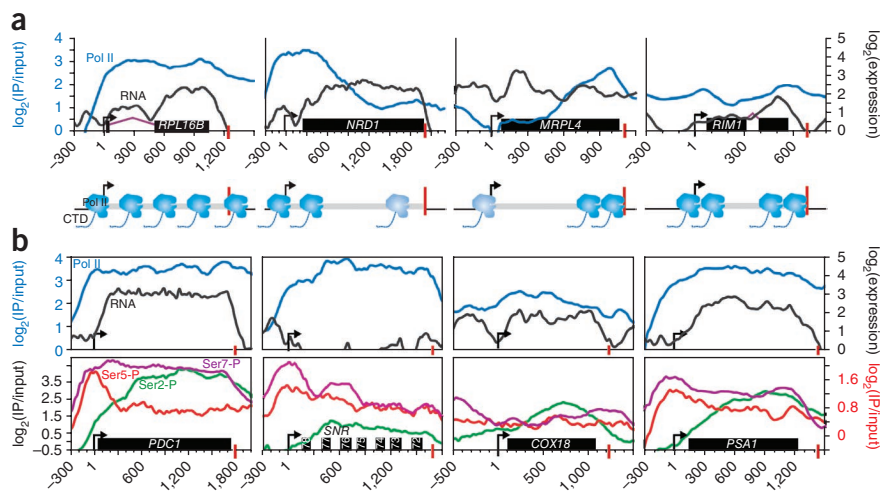
the Ser2-P marks are recognized in conjunction with the polyadenylation sequence by proteins involved in polyadenylation of the nascent transcript^{26–28}. During transcription termination, Fcp1 and Ssu72, two CTD phosphatases, dephosphorylate the CTD, making it available for the next cycle of transcription^{29–31}. In mammalian cells, Ser7-P marks are important for recruitment of the Integrator, a complex that plays an important role in 3’-processing of noncoding RNA^{32,33}. Whereas the substitution of this evolutionarily conserved residue with an alanine (S7A) has modest effects on growth, the substitution with a charged glutamate (S7E) is lethal^{34,35}. Thus, the placement and, more importantly, the removal of this phosphate moiety is critical in the transcription cycle.

The CTD code hypothesis posits that sequential CTD marks specify a recognition code in a manner akin to the histone code^{1–3,7,36,37}. Whether the patterns that underlie the CTD code are retained across different classes of genes in the genome remains a fundamentally important question. The observations that Ser2-P marks are not required for the expression of the p53-regulated p21 gene, histone genes or snRNA genes raises the specter that this mark is not universally needed for RNA synthesis^{38,39}. The early Ser5-P mark, thought to be essential for promoter release, is largely dispensable for mRNA synthesis^{8,40–42}. Despite its role in 3’-processing of noncoding genes^{32,34}, the Ser7-P mark is observed at promoters of all Pol II transcribed genes^{43–45}. It is unclear what role Ser7-P marks serve at protein-coding genes. Furthermore, the cross-talk between different modifications is an important but poorly understood phenomenon. Early experiments suggested that Ser5-P and Ser2-P modifications were placed independently²⁹. In fact, inhibition of one mark was shown to increase the abundance of the other, suggesting an antagonistic relationship⁴⁶. However, Ser5-P was recently shown to prime the CTD for subsequent phosphorylation of Ser2 by Bur1/Cdk9

¹Department of Biochemistry and The Genome Center, University of Wisconsin, Madison, Wisconsin, USA. ²Department of Epigenetics, Helmholtz Center Munich, Center of Integrated Protein Science, Munich, Germany. ³Department of Biostatistics & Medical Informatics, University of Wisconsin, Madison, Wisconsin, USA. ⁴Cellular and Molecular Pharmacology, University of California, San Francisco, San Francisco, California, USA. ⁵These authors contributed equally to this work. Correspondence should be addressed to A.Z.A. (ansari@biochem.wisc.edu).

Received 30 April; accepted 3 August; published online 29 August 2010; doi:10.1038/nsmb.1900

Figure 1 Pol II and CTD phosphorylation profiles. **(a)** ChIP-chip profiles for representative genes chosen to show the diversity of Pol II profiles across the genome. Blue, Pol II; black, total RNA; black boxes, translation boundaries; arrow and red bar, transcription boundaries (TSS and CPS, respectively). Introns are marked with a purple \wedge symbol. Scale on x axis, distance in bp from the TSS. Scale on y axis, fold enrichment of immunoprecipitation (IP) over input on a \log_2 scale for ChIP-chip data and fold expression over background for total RNA data. The cartoon beneath the plots shows the potential Pol II distributions that would yield the observed ChIP-chip occupancy profiles. **(b)** ChIP-chip profiles of genes for which Pol II occupancy profile (blue) is constant across the open reading frame (ORF). Purple, red and green, phosphorylation profiles (Ser7-P, Ser5-P and Ser2-P, respectively); black, total RNA.



(refs. 22,47,48). Notably, the interdependence and co-occurrence of Ser7-P is only now beginning to be explored. Thus, many questions about the universality of the sequential patterning of CTD marks remain to be resolved.

Our genome-wide analysis reveals an unexpected degree of co-occurrence of all three CTD marks, suggesting a bivalent or even multivalent mode of recognition by docking partners. A particularly unexpected observation is that Ser7-P is placed early in transcription and retained at robust levels until transcription termination. Chemical inhibition studies show that the promoter-distal Ser7-P marks are not remnants of early phosphorylation events but are replenished by Bur1. This defines a new role for Bur1 and suggests that Ser7-P marks are important for efficient transcription elongation. Finally, although we highlight the differential patterns of CTD marks at coding and noncoding genes, our genome-wide atlas of CTD marks serves as a general resource to identify new regulatory mechanisms that underlie the CTD code.

RESULTS

Genome-wide analyses reveal unexpected profiles

To explore the universality of the CTD code, we examined the occupancy profiles of Pol II and the three major CTD marks across the *S. cerevisiae* genome. We performed chromatin immunoprecipitation (ChIP) experiments and identified enriched DNA fragments via high-resolution tiled genomic microarrays (ChIP-chip). We immunoprecipitated Pol II using a monoclonal antibody against Rpb3, an integral subunit of the polymerase that is not influenced by CTD phosphorylation. We examined CTD phosphorylations using epitope-specific antibodies (see Online Methods for details). The high-resolution profiles revealed previously unknown patterns of Pol II association across some genes and confirmed known binding patterns at other genes (Fig. 1, traces in blue). For example, high occupancy of Pol II across the ribosomal protein gene *RPL16B* and rapid depletion of Pol II across the *NRD1* gene have been well documented⁴⁹ (Fig. 1a). By contrast, the enrichment of Pol II at the 3' end of the *MRPL4* gene or the enrichment at the 5' and 3' ends of the *RIM1* gene have not previously been observed (Fig. 1a). Although cryptic unstable transcripts (CUTs), stable unannotated transcripts (SUTs)^{50,51} and neighboring convergent genes may contribute to some of these profiles, there are some genes at which there is no neighboring or overlapping transcription to account for the 3'-enrichment of Pol II (Supplementary Fig. 2).

We then examined the genome-wide patterns of CTD phosphorylation. To ensure that the profiles of CTD modifications were not skewed by unusual Pol II profiles, we focused on genes bearing uniformly high levels of Pol II across the transcription unit (Fig. 1b). Particular examples include the protein-coding genes: *PDC1*, *COX18* and *PSA1*, as well as the noncoding polycistronic cluster *SNR78-72*. The Ser7-P profile across the *SNR* cluster is enriched at the 5' end of the gene, with dissipation of the signal toward the 3' end of the transcription unit. The protein-coding genes show different Ser7-P profiles. Unlike previous reports in human cells^{32,34}, we failed to detect Ser7-P enrichment solely in the middle of the coding region across the yeast genome.

By contrast, the reciprocal enrichment of Ser5-P at promoters and Ser2-P at the 3' ends is frequently observed and defines the current paradigm. However, the levels of Ser5-P across *COX18* and Ser2-P on the *SNR78-72* cluster do not conform to the paradigm and are lower than expected. The unexpected patterns of CTD marks at different genes are not due to experimental variability (Supplementary Fig. 3) but may arise from CUTs and SUTs.

Clustering genome-wide profiles of Pol II and CTD marks

To examine commonalities between patterns of Pol II and its modifications across the genome, we used an average transcription unit analysis (Fig. 2a). In this analysis, the entire transcription unit, from the transcription start site (TSS; Fig. 2a, arrow at 5' end) to the cleavage and polyadenylation site (CPS; Fig. 2a, vertical red bar at the 3' end), was represented by ten evenly scaled bins across all annotated genes in the genome (see Online Methods for details). The Pol II and CTD modification profiles are sorted by unrestrained *k*-means clustering, which partitions the genes into *k* clusters based on their ChIP-chip profiles. The profiles coalesce into four general clusters (Fig. 2b): uniform enrichment across the transcription unit (Fig. 2b, denoted by U), 5'-enrichment (Fig. 2b, denoted by 5), 3'-enrichment (Fig. 2b, denoted by 3) or 5'- and 3'-enrichments (Fig. 2b, denoted by 5+3). The four panels show the clustered profiles of Pol II and its modifications across all genes in the genome (Fig. 2b).

The compact nature of the yeast genome complicated the analysis due to signal bleeding over from neighboring genes and their regulatory elements. Therefore, we parsed the genes into three sets: the first (set I) included all 6,147 annotated genes in the genome, the second (set II) focused on 615 genes that have the highest levels (top 10%) of Pol II occupancy and the third (set III) is comprised of 60 genes

that show robust Pol II occupancy but are isolated from other known or predicted genes by at least 400 base pairs (bp). Notably, genes in set III are also devoid of overlapping or neighboring CUTs and SUTs. The profiles of Pol II and its modifications across the three sets of genes are summarized as pie charts (Fig. 2c).

The summary profiles of the 60 well-isolated protein-coding genes (set III) show that Ser7-P and Ser5-P marks are enriched at 5' end of genes (combining 5, 5+3 and U), whereas the Ser2-P mark is enriched at the 3' end of genes. A quantitative fit of the profiles show that Ser5-P and Ser7-P maxima occur within 50 bp of the start site, whereas the Ser2-P marks reach their first maxima by 517 ± 226 bp (Supplementary Fig. 4a,b). Unexpectedly, at ~36% of the genes, the

Ser5-P 'early' mark is also enriched at the 3' end (5+3 profile). The noncanonical enrichment of Ser5-P at the 3' ends and the occurrence of 'late' Ser2-P mark at the 5' ends of genes are unexpected. Moreover, only 15% of the set III genes show the canonical Ser5-P enrichment only at the 5' end followed by the reciprocal Ser2-P enrichment at the 3' end of transcription units. Thus, the accepted paradigm that Ser5-P is enriched only at promoters, Ser7-P in the middle of the coding regions and Ser2-P toward the end does not adequately describe the patterns of CTD marks observed across the genome, and the paradigm, therefore, should be revised.

To assess the functional importance of Ser7-P profiles, we examined gene ontology enrichment within each cluster. We refined the

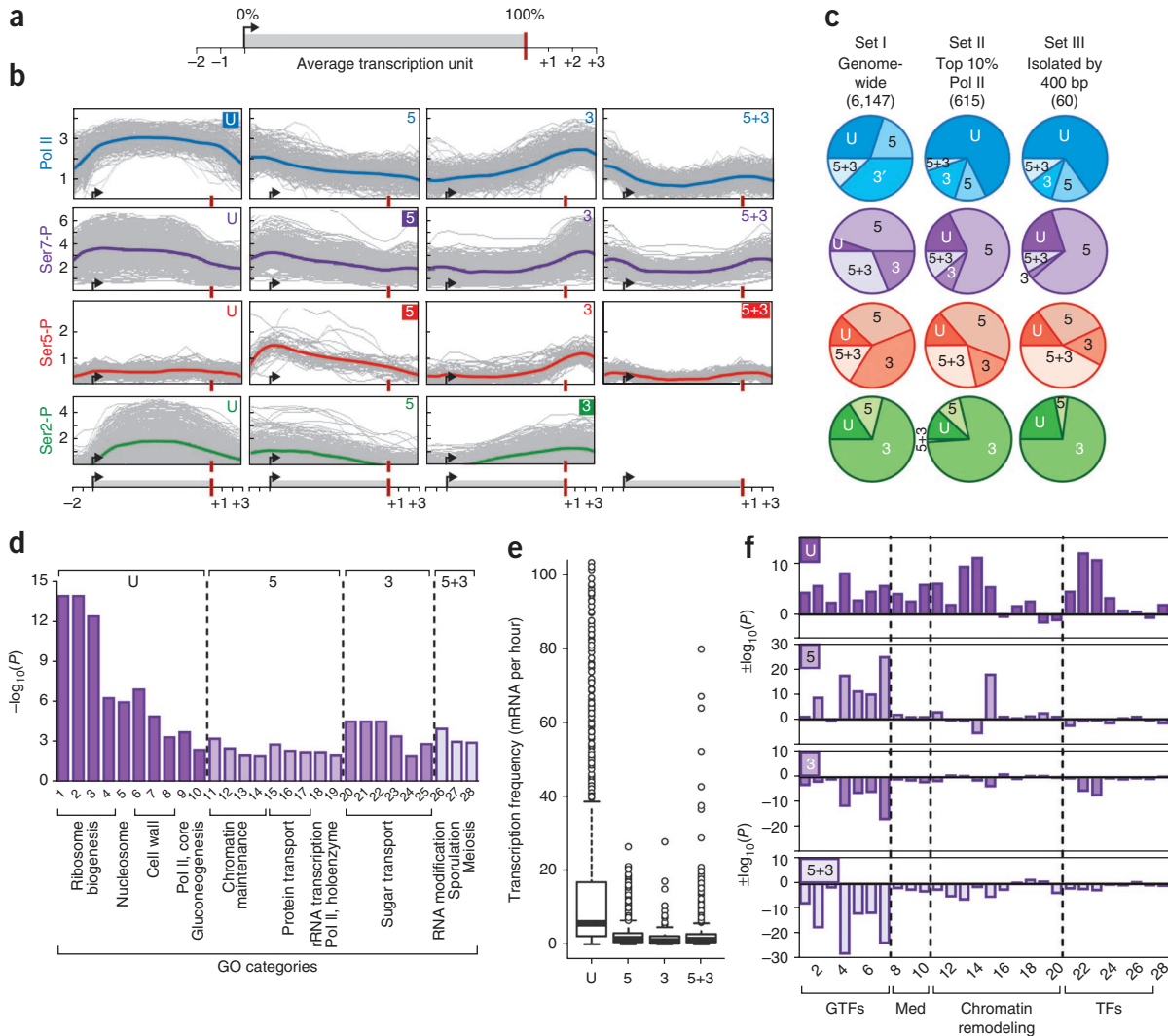
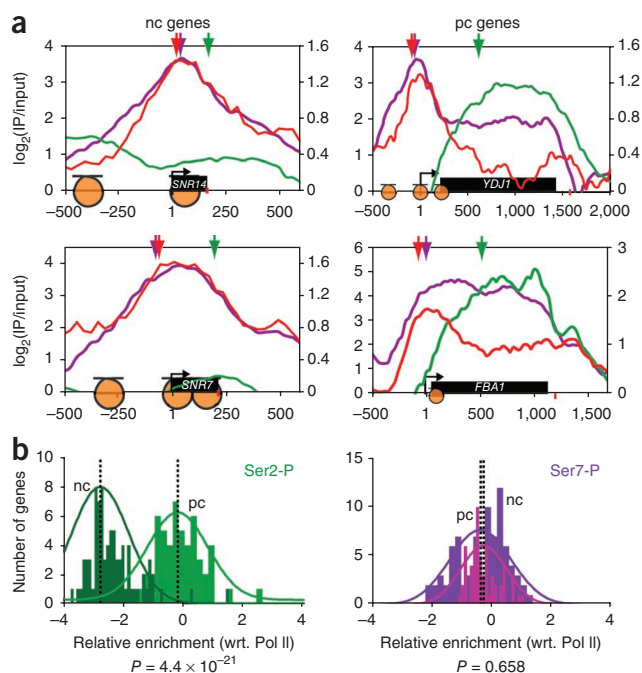


Figure 2 Genome-wide Pol II and CTD phosphorylation profiles. (a) The diagram summarizes the scale used in the average transcription unit analysis. Bins within transcribed region are equivalent to 10% of the transcribed region length, and bins flanking this region (−1, +1) are a constant 157 bp. (b) Representative clusters from the k-means clustering analysis for Pol II, Ser7-P, Ser5-P and Ser2-P occupancy profiles across the genome using average transcription unit analysis (see Online Methods). U, uniform enrichment across the transcription unit; 5, 5' enrichment; 3, 3' enrichment; 5+3, 5' and 3' enrichments. The dominant profile(s) for each is highlighted. (c) Pie chart diagrams showing the distribution of genes within each gene set for Pol II, Ser7-P, Ser5-P and Ser2-P having each of the profiles shown in b. Set I, annotated protein-coding genes (6,147 genes); set II, protein-coding genes with an average Pol II enrichment in the top 10% (615 genes); set III, protein-coding genes isolated by 400 bp and having an average Pol II enrichment greater than or equal to 1 (60 genes). (d) Histogram of significantly enriched gene ontology (GO) categories within individual Ser7-P clusters (U, 5, 3 and 5+3). Details for each GO category are provided in Supplementary Table 1. (e) Box plots of transcription frequency for genes within each Ser7-P cluster⁵². The uniform (U) Ser7-P cluster is strongly enriched for genes with higher rates of transcription frequency compared to the genome average ($P = 3.35 \times 10^{-30}$). (f) Bar graph of transcription machinery at the upstream activating sequence within individual Ser7-P clusters. The individual proteins are listed in Supplementary Figure 6. Proteins that are enriched within the cluster are represented by positive $\log_{10}(P)$ values, whereas proteins that are depleted are represented by negative $\log_{10}(P)$ values⁵³. Dashed lines segregate the components of each complex. GTFs, general transcription factors; Med, Mediator complex; TFs, transcription factors.

Figure 3 CTD phosphorylation profile for protein-coding and noncoding genes. (a) Phosphorylation profiles across several representative noncoding (nc) genes (left column) and protein-coding (pc) genes (right column). Color-coded arrows, respective phosphorylation peak. The noncoding genes show overlapping Ser5-P (red) and Ser7-P (purple) profiles, whereas varying levels of 3' Ser7-P enrichment are observed in protein-coding genes. Ser2-P (green) appears to be less abundant in noncoding genes. Orange circles, nucleosome positions near the TSS⁶⁰ (drawn to scale). (b) Histograms showing the relative enrichment (with respect to Pol II levels) across noncoding and protein-coding genes for Ser7-P and Ser2-P. The Ser2-P levels are significantly lower in noncoding genes than protein-coding genes ($P = 4.4 \times 10^{-21}$). No significant difference in Ser7-P was detected between noncoding and protein-coding genes ($P = 0.658$).



clusters obtained using k-means using silhouette analysis, in which scores were assigned to the genes within each cluster. A silhouette score gives a measure of how well a gene profile fits in a given cluster. Iterative optimization allowed us to obtain the highest-confidence genes for each cluster (Supplementary Fig. 5). We then examined the clusters to find groups of ontologically related genes unique to each cluster (Fig. 2d, Supplementary Fig. 6 and Supplementary Table 1). The strong enrichment of ribosomal biogenesis genes with the uniform Ser7-P profile was especially striking ($P < 10^{-14}$). To further validate this result, we performed a hypergeometric comparison of genes within the uniform cluster with known genome-wide binding sites of all yeast transcription factors. Consistent with the gene ontology enrichment, transcription factors involved in ribosome biogenesis (*FHL1*, *RAP1* and *SFP1*) were significantly enriched in the uniform cluster (Supplementary Fig. 6a). To examine the generality of our initial observations, we compared the known rates of RNA synthesis for genes within each cluster⁵². The uniform cluster was enriched for highly transcribed genes. The reciprocal analysis of the genes transcribed at the highest frequency revealed that 86% had the uniform Ser7-P profile. (Fig. 2e and Supplementary Fig. 6c). Further comparison with genome-wide maps of components of the transcriptional machinery, chromatin remodeling machines and transcription factors revealed that genes within the uniform cluster were highly enriched for factors that stimulate high levels of transcription⁵³ (Fig. 2f and Supplementary Fig. 7). In essence, multiple analyses of datasets from independent sources tie the highly expressed genes to uniform patterns of Ser7-P marks across the transcribed regions. Thus, the Ser7-P mark may contribute to efficient transcription elongation.

Distinct patterns at noncoding versus protein-coding genes

Ser7-P is only thought to be important for 3'-processing of snRNA; however, it is also placed robustly at protein-coding genes. It is unknown what role this CTD mark may serve at protein-coding genes. We therefore examined whether the patterns of CTD marks differ between noncoding and protein-coding genes (Fig. 3a). The Ser7-P and Ser5-P profiles on *SNR7* and *SNR14* are strikingly similar, but they differ from the profiles at protein-coding genes (*YDJ1* and *FBA1* in Fig. 3a). At protein-coding genes, Ser7-P and Ser5-P profiles coincide at the promoter but rapidly deviate within coding regions. Whereas Ser5-P levels abate, Ser7-P levels are retained at high levels until the 3' end. Moreover, markedly lower levels of Ser2-P are apparent across noncoding genes when compared to those of protein-coding genes. None of the profiles show any correlation with the well-positioned nucleosomes at promoters of genes (Fig. 3a).

To extend the comparison beyond a few representative genes, we calculated the average levels of Ser7-P and Ser2-P marks for the 82 noncoding genes (small nuclear RNA (snRNA) and small nucleolar

RNA) transcribed by Pol II and the 60 protein-coding genes of set III (from Fig. 2b). Other than distance from neighboring genes, the set III protein-coding genes are ontologically unrelated to each other, and they provide unambiguous occupancy profiles. The genome-scale data clearly show that the extent of Ser7-P modification on both classes of genes is equivalent. However, the levels of Ser2-P are 400% lower on noncoding genes ($P = 4.4 \times 10^{-21}$) (Fig. 3b). Even when correcting for the shorter size of noncoding genes, we find that the levels of Ser2-P are 275% lower than the signals observed within the first 300 bp of protein-coding genes ($P = 1.9 \times 10^{-10}$) (Supplementary Fig. 4c). The lower levels of Ser2-P marks and the abundance of Ser7-P at noncoding genes likely serve as a signal for enzymes that process noncoding transcripts.

Chemical-genomics reveals cross-talk between CTD marks

To examine the cross-talk between the CTD marks, we used a chemical-genetic approach to inhibit the two major kinases that phosphorylate Ser5 during transcription initiation: transcription factor IIH-associated Kin28/Cdk7 and, to a lesser extent, the Mediator-associated Srb10/Cdk8 (refs. 8,40) (Supplementary Fig. 8a). To inhibit these two kinases selectively, their ATP binding pockets were genetically altered to accept cell-permeable inhibitor analogs^{8,54} (Supplementary Fig. 8a). Consistent with our previous studies, targeted chemical inhibition of Kin28/Cdk7 in combination with Srb10/Cdk8 (Kin28as + Srb10as) blocks a significant portion of the kinase activity and leads to a rapid decrease in cell growth^{8,40} (Supplementary Fig. 8a). Chemical inhibition of Kin28as + Srb10as *in vivo* leads to a precipitous decrease in Ser5-P marks at the 5' end of several genes (*SED1* in Fig. 4a). Unexpectedly, under similar treatment, Ser7-P marks are only attenuated at the promoter. The promoter-proximal loss of both marks is particularly evident upon normalization to Pol II (Supplementary Fig. 8b).

To further clarify the remodeling of occupancy patterns, we examined the genes in set II that show uniformly high levels of Pol II occupancy throughout the transcription unit (Fig. 4b). The profiles from the untreated and the chemically inhibited double mutant strain were binned as described above (see Fig. 2). The mean of 415 genes is shown

Figure 4 Small-molecule inhibition of CTD phosphorylation. (a) Inhibition effects on total RNA (black), Pol II (blue), Ser7-P (purple), Ser5-P (red) and Ser2-P (green) occupancy profiles for *SED1*. Solid line, uninhibited profiles; dashed line, inhibited profiles. (b) Summary of average Kin28as + Srb10as responses to inhibition for Pol II (blue), Ser7-P (purple), Ser5-P (red) and Ser2-P (green). Data shown for 415 genes with 'uniform' Pol II profiles from set II in the wild-type strain (see **Supplementary Fig. 9**, central Pol II pie). Solid and dashed lines, uninhibited and inhibited Kin28as + Srb10as average profiles, respectively. Scale on the x axis is shown as distance from the TSS using average transcription unit analysis (described in **Fig. 2a**). Scale on y axis represents fold enrichment of immunoprecipitation over input on a log₂ scale. (c) Comprehensive diagrams showing the comparison between the uninhibited wild-type strain (large central pies) and the inhibited double-mutant strain (smaller pies) for all the genes in set III (described in **Fig. 2c**). Summaries shown for Pol II (blue), Ser7-P (purple), Ser5-P (red) and Ser2-P (green). The smaller pie charts correspond to a slice of the wild-type chart and show the partitioning of the genes from the double-mutant data within that slice after the inhibitor was added. The profiles U, 5, 3 and 5+3 are as described in **Figure 2**, and I is used to indicate the profiles seen after inhibition (IU, I⁵, I³, and I⁵⁺³).

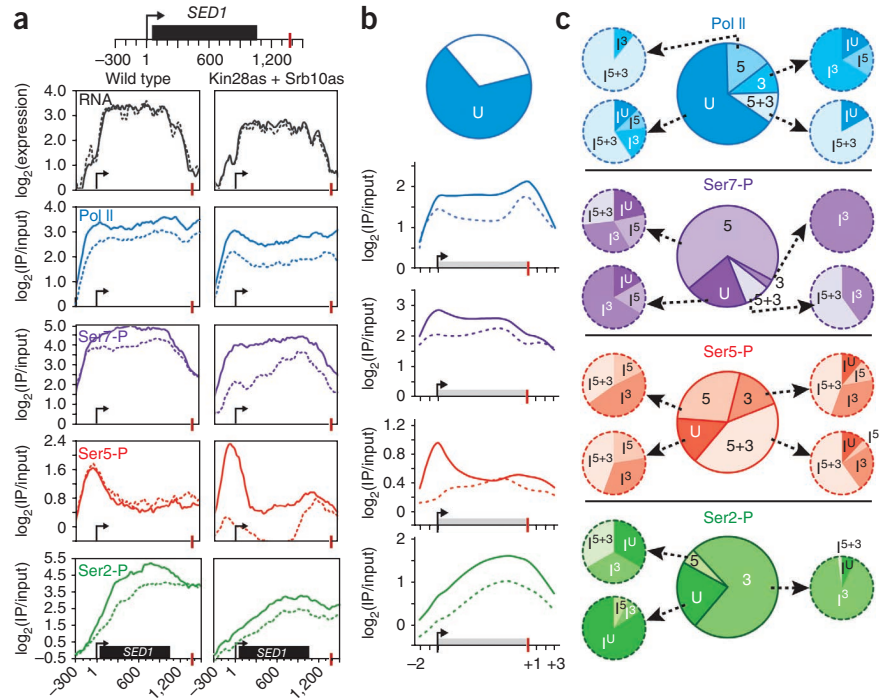


(**Fig. 4b**). Upon inhibition, the Pol II profile shows a clear decrease in the middle of the coding region, resulting in a bimodal distribution with peaks at the 5' and 3' ends of the transcription unit (profile I⁵⁺³). Ser5-P and Ser7-P marks are markedly reduced at 5' ends, but they are unperturbed within coding regions. In agreement with recent reports^{47,48}, this decrease in Ser5-P leads to a subtle but detectable

decrease in Ser2-P. However, it is noteworthy that, in contrast to Ser5-P and Ser7-P, the overall profile of the Ser2-P mark does not change.

We then examined the consequences of inhibiting Kin28as + Srb10as across the genome (**Fig. 4c** and **Supplementary Fig. 9**). The profile clusters for the inhibited strain resemble those seen previously (U, 5, 3, 5+3), but they were labeled with an 'I' (inhibitor-treated) to

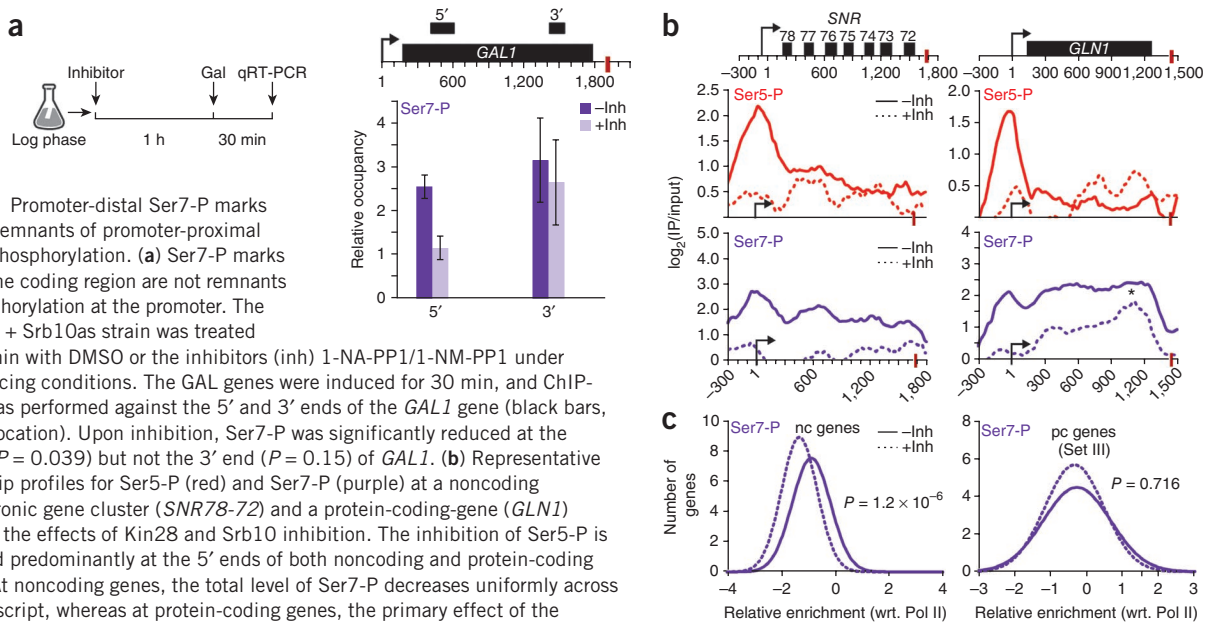


Figure 5 Promoter-distal Ser7-P marks are not remnants of promoter-proximal Kin28 phosphorylation. (a) Ser7-P marks within the coding region are not remnants of phosphorylation at the promoter. The Kin28as + Srb10as strain was treated for 60 min with DMSO or the inhibitors (inh) 1-NA-PP1/1-NM-PP1 under noninducing conditions. The GAL genes were induced for 30 min, and ChIP-qPCR was performed against the 5' and 3' ends of the *GAL1* gene (black bars, primer location). Upon inhibition, Ser7-P was significantly reduced at the 5' end ($P = 0.039$) but not the 3' end ($P = 0.15$) of *GAL1*. (b) Representative ChIP-chip profiles for Ser5-P (red) and Ser7-P (purple) at a noncoding polycistronic gene cluster (*SNR78-72*) and a protein-coding gene (*GLN1*) showing the effects of Kin28 and Srb10 inhibition. The inhibition of Ser5-P is observed predominantly at the 5' ends of both noncoding and protein-coding genes. At noncoding genes, the total level of Ser7-P decreases uniformly across the transcript, whereas at protein-coding genes, the primary effect of the inhibition is seen at the 5' end of the transcript. This suggests the presence of a secondary Ser7 kinase acting near the 3' end of protein-coding genes (indicated by an asterisk (*)). (c) Histogram showing the effects of inhibition on the relative Ser7-P enrichment (with respect to Pol II levels) at the 3' end of the ORF of noncoding (nc) genes (left) and protein-coding (pc) genes (right). (noncoding genes, $P = 1.2 \times 10^{-6}$; protein-coding genes, $P = 0.716$).

decrease in Ser2-P. However, it is noteworthy that, in contrast to Ser5-P and Ser7-P, the overall profile of the Ser2-P mark does not change. We then examined the consequences of inhibiting Kin28as + Srb10as across the genome (**Fig. 4c** and **Supplementary Fig. 9**). The profile clusters for the inhibited strain resemble those seen previously (U, 5, 3, 5+3), but they were labeled with an 'I' (inhibitor-treated) to

© 2010 Nature America, Inc. All rights reserved.



differentiate them from the clusters from the untreated wild-type strain (Figs. 2c and 4c). Using this nomenclature, we compared the profiles from wild-type strains (central pie charts, U, 5, 3, 5+3) with the profiles for the same genes in the chemically inhibited Kin28as + Srb10as strain (surrounding pie charts: I^U, I⁵, I³, I⁵⁺³; Fig. 4c and Supplementary Fig. 9). The inhibition data for Pol II is striking, as a significant fraction of genes from the uniform and 5'-enriched clusters (U, 5) are altered to the 5'+3' enriched profile (I⁵⁺³ in dashed circles). In addition, the Ser7-P profiles are remodeled with a loss of 5'-enriched patterns and an increase of 3'-enrichment (I³) within the coding regions. Ser5-P profiles are also remodeled, as the 5'-enrichment is lost. The 3'-enriched fraction of Ser2-P profiles is not substantially altered. Taken together, the data indicate that promoter-proximal Ser5-P and Ser7-P marks are strongly coupled, whereas promoter-distal Ser2-P and Ser7-P marks are not strictly dependent on early CTD marks. The coupling of Ser5-P and Ser7-P at promoters is consistent with the role of Kin28/Cdk7 in phosphorylating these residues⁴³⁻⁴⁵. However, the occurrence of Ser7-P within coding regions is unexpected.

An internal Ser7 kinase acts within coding regions of genes

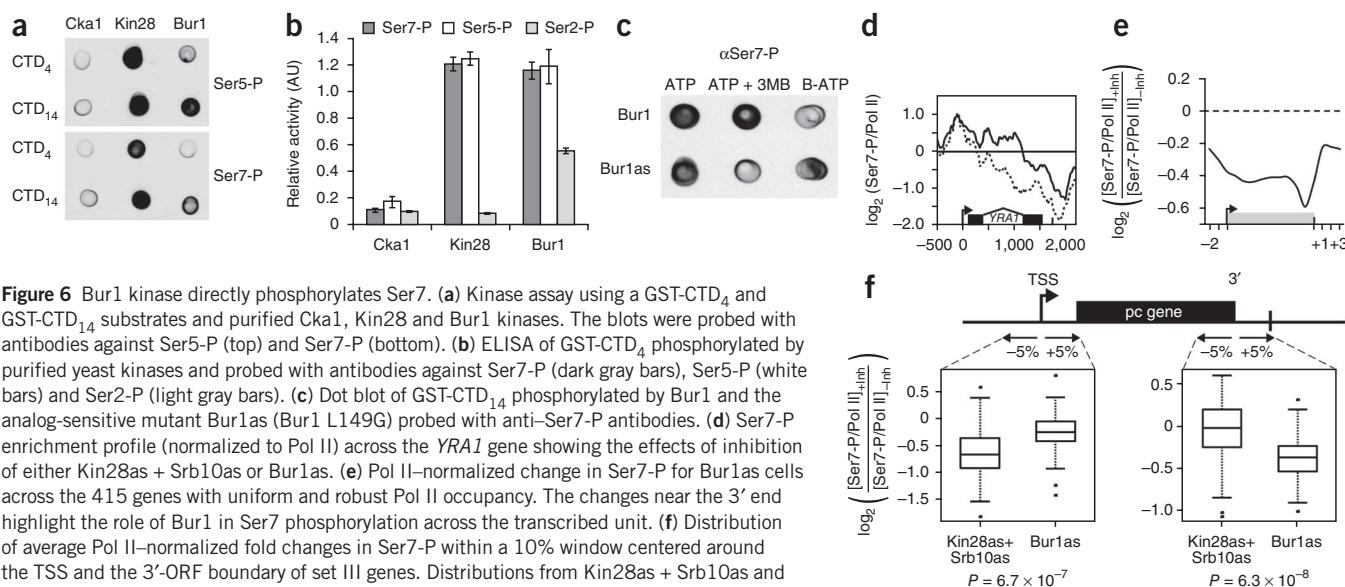
To determine whether Ser7-P marks detected within coding regions are not remnants of marks placed at the promoter, we examined the distribution of this mark at the inducible *GAL1* gene. We first inhibited Kin28as + Srb10as for 60 min in noninducing conditions. Under these conditions, we detect no Pol II at the *GAL1* promoter and have previously shown that both Kin28as and Srb10as remain chemically inhibited^{8,40}. Next, we induced the *GAL* genes for 30 min and used ChIP with quantitative PCR (ChIP-qPCR) to examine the distribution of Pol II and Ser7-P marks at the 5' and 3' ends of the *GAL1* gene (Fig. 5a). The data reveal an unambiguous diminution of Ser7-P marks at the 5' end and a robust signal for this mark at the 3' end. In other words, the internal Ser7-P marks are placed anew by a different kinase(s): one that is not sensitive to inhibitors of Kin28as and Srb10as.

To explore whether internal Ser7-P marks are also placed anew in noncoding genes, we compared the changes in the Ser7-P profiles at protein-coding and noncoding genes that are of similar length and have similar polymerase occupancy. The *SNR78-72* polycistronic cluster and *GLN1* gene show comparable levels of Ser7-P and Ser5-P marks at the promoter and are equally responsive to the inhibitor at the

5' end (Fig. 5b). However, in contrast to *GLN1*, Ser7-P marks are not replenished at the 3' end of the *SNR78-72* cluster. We systematically examined the levels of Ser7-P marks at the 3' end of 82 noncoding genes and the 60 protein-coding genes from set III (Fig. 5c). The data unambiguously show that inhibiting promoter-proximal kinases leads to a loss of Ser7-P at noncoding genes but not at protein-coding genes. Thus, chemical-genomic analysis reveals the existence of a Ser7 kinase that acts on elongating polymerases.

To identify the internal Ser7 kinase, we purified the four kinases that phosphorylate the CTD during different stages of transcription: Kin28/Cdk7, Srb10(Srb11)/Cdk8, Bur1/Cdk9 and Ctk1/Cdk9 (Supplementary Fig. 1). Consistent with our previous work, Kin28 phosphorylates Ser5 and Ser7 residues on a GST fusion protein bearing four or more heptapeptide repeats⁴³ (Fig. 6a). Whereas Bur1 does not phosphorylate substrates bearing 3 heptapeptide repeats⁵⁴, it phosphorylates Ser7 on substrates bearing 4 or 14 repeats (Fig. 6a). Our results are consistent with recent reports of Bur1 preferentially phosphorylating longer CTD substrates³⁷. The kinase activity was quantified using an ELISA (Fig. 6b). Notably, neither Srb10 nor the control Cka1 kinase phosphorylates Ser7 in parallel assays (Fig. 6a and Supplementary Fig. 10a).

To validate these observations, we used a strain in which we engineered Bur1 to bind a bulky purine analog, 3-MB-PP1 (ref. 22). Unlike the wild-type enzyme, the enlarged ATP binding site of the engineered Bur1 (Bur1as) is inhibited by 3-MB-PP1 and can utilize the bulky ATP analog N⁶-benzyl-ATP to phosphorylate Ser7 *in vitro* (Fig. 6c). The inhibitor has only a modest effect on the growth rate of Bur1as cells, suggesting a partial *in vivo* inhibition of this kinase whose function is vital for cell viability (Supplementary Fig. 10b). However, this degree of inhibition is sufficient to reduce the ability of Bur1 to modify Spt5 or CTD *in vivo*^{22,48}. In agreement with its *in vitro* activity, chemical inhibition of the Bur1as strain led to a loss of Ser7-P marks *in vivo* at the *SNR* cluster and *GLN1* (Supplementary Fig. 10d). This loss of Ser7-P within the coding region is not observed in chemically treated isogenic wild-type strain or the Kin28as + Srb10as strain (Supplementary Fig. 10c). In contrast, the loss of Ctk1 nearly abolishes Ser2-P marks but has no effect on Ser7-P at the *SNR* cluster and the internal site of *GLN1*. The decrease in Ser7-P levels at *GLN1* in the *ctk1Δ* strain may result from



latent Ser7-P activity of this kinase *in vivo* or the inability of Pol II to release basal transcription factors in the absence of Ctk1 (ref. 55).

To examine the genome-wide contribution of Bur1 to Ser7-P profiles, we performed ChIP-chip analysis on the Bur1as strain in the presence or absence of the inhibitor. Unlike the promoter-proximal decrease in Ser7-P upon inhibition of Kin28as + Srb10as, inhibition of Bur1 reduces Ser7-P within the coding region (Fig. 6d). The summarized data on genes in set II with uniformly Pol II profiles show that the decrease is most apparent within the coding region, with the greatest effect toward the 3' end (Fig. 6e). Moreover, a direct comparison of changes in Ser7-P levels upon chemical inhibition of Kin28as + Srb10as or Bur1as further highlights the role of Kin28 at the 5' end and Bur1 at the 3' end of genes (Fig. 6f). The results are consistent with the ability of Bur1 to act on elongating polymerases from promoter-proximal regions until the 3' end of genes.

DISCUSSION

This study provides the first genome-wide atlas to our knowledge of CTD modifications that orchestrate stage-specific processes in RNA biogenesis. The data reveal (i) ubiquitous co-occurrence of CTD marks across the transcribed units, (ii) the existence of gene class-specific patterns of Pol II and its modifications, (iii) weak coupling between promoter-proximal and promoter-distal CTD marks, (iv) that Ser7-P marks within coding regions are placed anew and are not remnants of marks placed by Kin28 at the promoter and (v) a novel role of Bur1 as a Ser7 kinase that acts on elongating Pol II. Taken together, our data suggest that accepted paradigms underlying the CTD code should be revised to accommodate combinatorial patterns of CTD modifications.

The widespread co-occurrence of CTD marks does not mean that they are placed at equivalent levels at all genes across the genome. We observe distinct patterns of the three marks between noncoding and protein-coding genes. Ser7-P closely mirrors the patterns of Ser5-P across the entire noncoding gene, whereas at protein-coding genes, the Ser7-P mark persists well beyond the point where Ser5-P levels drop markedly. Moreover, Ser2-P marks are underrepresented at noncoding genes, even when the length of the transcript is taken into consideration. The distinct patterns of CTD marks at these two gene classes reflect the different mechanisms of transcription termination and 3'-end processing that act on these two classes of RNA^{49,56–59}.

The co-occurrence of CTD marks is consistent with our observation that two kinases known to phosphorylate the CTD also place bivalent marks. We and others previously identified the ability of Kin28/Cdk7 to phosphorylate Ser5 and Ser7 (refs. 43–45). Because Kin28/Cdk7 associates with Pol II at promoters, the co-occurrence of Ser5 and Ser7 marks within 50 bp of the TSS can be ascribed to the action of Kin28/Cdk7. We also show that Srb10, another Ser5 kinase, does not contribute to Ser7-P marks at promoters or within coding regions (Fig. 4). Inhibition of Kin28as + Srb10as revealed, for the first time to our knowledge, the existence of other kinases that act on Ser7 residues of the elongating polymerase. A series of kinase assays on CTD substrates bearing more than three heptapeptide repeats revealed that Bur1 phosphorylates Ser7. The requirement for longer CTD substrates was previously noted in studies that examined the ability of Bur1 to phosphorylate Ser2 (ref. 48). The inhibition of Bur1as with cell-permeable inhibitors further confirmed its role as a Ser7-P kinase *in vivo* (Fig. 6d,e and Supplementary Fig. 10c,d). This is a previously unknown role for Bur1, one that couples the placement of Ser7-P with Ser2-P on elongating polymerases.

In performing these experiments, we were surprised to find that promoter-distal Ser7-P marks were not eliminated by inhibition of the

promoter-proximal Ser7 kinase. This observation is inconsistent with the notion that promoter-distal Ser7-P marks were remnants of the marks placed by Kin28 at the promoter. Similarly, promoter-distal Ser2-P and Ser5-P marks were not eliminated upon simultaneous inhibition of promoter-proximal Ser5 kinases (Srb10 and Kin28). Moreover, it was recently suggested that promoter-proximal Ser5-P marks were critical for sequential placement of Ser2-P marks on the elongating Pol II. Thus, contrary to the expectation that early marks prime the CTD for subsequent modifications, our data indicate that promoter-distal placement of CTD modifications is not acutely dependent on early marks.

Previous mutational analyses highlight the importance of dynamic placement of Ser7-P marks. The substitution of Ser7 with a glutamate (S7E) is lethal, whereas the inability to phosphorylate this position (S7A in T4A containing CTDs) only results in a decreased growth rate at suboptimal temperatures^{34,35}. The removal and replenishment of Ser7-P marks within coding regions may serve as a critical signal for the exchange of factors during the transition from promoter release to productive elongation. A role for Ser7-P in efficient elongation is consistent with the observation that highly transcribed genes show high levels of this CTD mark. Moreover, the ability of Bur1 to place this mark is consistent with its ability to associate with transcribing Pol II and stimulate transcriptional elongation^{24,25}. In addition to improving elongation via phosphorylation of Spt5 (refs. 22,23), Bur1-mediated placement of Ser7-P marks could help recruit cellular machinery that facilitates elongation and suppresses cryptic transcripts. This could well explain why Ser7-P marks are observed across all protein-coding genes even though their function is only defined at noncoding genes.

METHODS

Methods and any associated references are available in the online version of the paper at <http://www.nature.com/nsmb/>.

Accession codes. ArrayExpress: Data has been deposited under the accession number E-MEXP-2850.

Note: Supplementary information is available on the Nature Structural & Molecular Biology website.

ACKNOWLEDGMENTS

We thank S. Hahn (Fred Hutchinson Cancer Research Center) for sharing strains before publication and for helpful discussions, J. Nau and A. Nett for optimizing strains, E. Kanin and A. Leaf for exploratory experiments, D. Burgess and N. Thompson (Univ. of Wisconsin-Madison) for the gift of Pol II antibody (RPB3) and C. Zhang (Univ. of California, San Francisco) for providing small-molecule inhibitors and for their advice on the kinase inhibition experiments. We also gratefully acknowledge the support of the US National Science Foundation (MCB 07147), W.M. Keck, Shaw Scholar and Vilas Associate awards (to A.Z.A.), J.R.T. and J.B.R.-M. were supported by a US National Human Genome Research Institute training grant to the Genomic Sciences Training Program (5T32HG002760). D.E. was supported by Deutsche Forschungsgemeinschaft SFB/TR5 and SFB684 and S.K. was supported by HG03747 (US National Institutes of Health). M.H. was funded by a Boehringer Ingelheim Fonds travel grant.

AUTHOR CONTRIBUTIONS

J.R.T., D.W.Z. and B.E.W. performed the ChIP-chip experiments in the JTY1 and Kin28as + Srb10as strains; J.B.R.-M. performed the ChIP-chip experiments with the BY4743 and Bur1as strains; J.R.T. analyzed the ChIP-chip data for all the experiments; M.S.A. and D.W.Z. performed the kinase assays; X.L. and S.K. assisted with data analysis; M.H. performed the ELISA assays; A.Z.A., R.D.C. and D.E. planned and analyzed the Ser7-P experiments; K.S. provided the unpublished small-molecule inhibitors and assisted in the planning of the kinase inhibition experiments; J.R.T., D.W.Z., J.B.R.-M. and A.Z.A. wrote the manuscript; all authors commented on the manuscript.

COMPETING FINANCIAL INTERESTS

The authors declare competing financial interests: details accompany the full-text HTML version of the paper at <http://www.nature.com/nsmb/>.

Published online at <http://www.nature.com/nsmb/>.

Reprints and permissions information is available online at <http://npg.nature.com/reprintsandpermissions/>.

1. Phatnani, H.P. & Greenleaf, A.L. Phosphorylation and functions of the RNA polymerase II CTD. *Genes Dev.* **20**, 2922–2936 (2006).
2. Buratowski, S. The CTD code. *Nat. Struct. Biol.* **10**, 679–680 (2003).
3. Corden, J.L. Transcription: seven ups the code. *Science* **318**, 1735–1736 (2007).
4. Perales, R. & Bentley, D. “Cotranscriptionality”: the transcription elongation complex as a nexus for nuclear transactions. *Mol. Cell* **36**, 178–191 (2009).
5. Lee, T.I. & Young, R. Transcription of eukaryotic protein-coding genes. *Annu. Rev. Genet.* **34**, 77–137 (2000).
6. Myers, L.C. & Kornberg, R.D. Mediator of transcriptional regulation. *Annu. Rev. Biochem.* **69**, 729–749 (2000).
7. Sims, R.J. III, Belotserkovskaya, R. & Reinberg, D. Elongation by RNA polymerase II: the short and long of it. *Genes Dev.* **18**, 2437–2468 (2004).
8. Liu, Y. *et al.* Two cyclin-dependent kinases promote RNA polymerase II transcription and formation of the scaffold complex. *Mol. Cell. Biol.* **24**, 1721–1735 (2004).
9. Ansari, A.Z., Ogirala, A. & Ptashne, M. Transcriptional activating regions target attached substrates to a cyclin-dependent kinase. *Proc. Natl. Acad. Sci. USA* **102**, 2346–2349 (2005).
10. Riedl, T. & Egly, J.M. Phosphorylation in transcription: the CTD and more. *Gene Expr.* **9**, 3–13 (2000).
11. Max, T., Sogaard, M. & Svejstrup, J. Hyperphosphorylation of the C-terminal repeat domain of RNA polymerase II facilitates dissociation of its complex with mediator. *J. Biol. Chem.* **282**, 14113–14120 (2007).
12. Schroeder, S.C., Schwer, B., Shuman, S. & Bentley, D. Dynamic association of capping enzymes with transcribing RNA polymerase II. *Genes Dev.* **14**, 2435–2440 (2000).
13. Komarnitsky, P., Cho, E.J. & Buratowski, S. Different phosphorylated forms of RNA polymerase II and associated mRNA processing factors during transcription. *Genes Dev.* **14**, 2452–2460 (2000).
14. Ng, H.H., Robert, F., Young, R.A. & Struhl, K. Targeted recruitment of Set1 histone methylase by elongating Pol II provides a localized mark and memory of recent transcriptional activity. *Mol. Cell* **11**, 709–719 (2003).
15. Krogan, N.J. *et al.* Methylation of Histone H3 by Set2 in *Saccharomyces cerevisiae* is linked to transcriptional elongation by RNA polymerase II. *Mol. Cell. Biol.* **23**, 4207–4218 (2003).
16. Carrozza, M.J. *et al.* Histone H3 methylation by Set2 directs deacetylation of coding regions by Rpd3S to suppress spurious intragenic transcription. *Cell* **123**, 581–592 (2005).
17. Mosley, A.L. *et al.* Rtr1 is a CTD phosphatase that regulates RNA polymerase II during the transition from serine 5 to serine 2 phosphorylation. *Mol. Cell* **34**, 168–178 (2009).
18. Brès, V., Yoh, S. & Jones, K. The multi-tasking P-TEFb complex. *Curr. Opin. Cell Biol.* **20**, 334–340 (2008).
19. Buratowski, S. Progression through the RNA polymerase II CTD cycle. *Mol. Cell* **36**, 541–546 (2009).
20. Kornblihtt, A.R., De La Mata, M., Fededa, J., Munoz, M. & Noguez, G. Multiple links between transcription and splicing. *RNA* **10**, 1489–1498 (2004).
21. Wood, A. & Shilatifard, A. Bur1/Bur2 and the Ctk complex in yeast: the split personality of mammalian P-TEFb. *Cell Cycle* **5**, 1066–1068 (2006).
22. Liu, Y. *et al.* Phosphorylation of the transcription elongation factor Spt5 by yeast Bur1 kinase stimulates recruitment of the PAF complex. *Mol. Cell. Biol.* **29**, 4852–4863 (2009).
23. Zhou, K., Kuo, W., Fillingham, J. & Greenblatt, J. Control of transcriptional elongation and cotranscriptional histone modification by the yeast BUR kinase substrate Spt5. *Proc. Natl. Acad. Sci. USA* **106**, 6956–6961 (2009).
24. Chu, Y., Simic, R., Warner, M., Arndt, K. & Prelich, G. Regulation of histone modification and cryptic transcription by the Bur1 and Paf1 complexes. *EMBO J.* **26**, 4646–4656 (2007).
25. Keogh, M.C., Podolny, V. & Buratowski, S. Bur1 kinase is required for efficient transcription elongation by RNA polymerase II. *Mol. Cell. Biol.* **23**, 7005–7018 (2003).
26. Proudfoot, N.J., Furger, A. & Dye, M.J. Integrating mRNA processing with transcription. *Cell* **108**, 501–512 (2002).
27. Licatalosi, D.D. *et al.* Functional interaction of yeast pre-mRNA 3′ end processing factors with RNA polymerase II. *Mol. Cell* **9**, 1101–1111 (2002).
28. Ahn, S.H., Kim, M. & Buratowski, S. Phosphorylation of serine 2 within the RNA polymerase II C-terminal domain couples transcription and 3′ end processing. *Mol. Cell* **13**, 67–76 (2004).
29. Cho, E.J., Kobar, M.S., Kim, M., Greenblatt, J. & Buratowski, S. Opposing effects of Ctk1 kinase and Fcp1 phosphatase at Ser 2 of the RNA polymerase II C-terminal domain. *Genes Dev.* **15**, 3319–3329 (2001).
30. Krishnamurthy, S., He, X., Reyes-Reyes, M., Moore, C. & Hampsey, M. Ssu72 is an RNA polymerase II CTD phosphatase. *Mol. Cell* **14**, 387–394 (2004).
31. Steinmetz, E.J., Conrad, N., Brow, D. & Corden, J. RNA-binding protein Nrd1 directs poly (A)-independent 3′-end formation of RNA polymerase II transcripts. *Nature* **413**, 327–331 (2001).
32. Egloff, S. *et al.* Serine-7 of the RNA polymerase II CTD is specifically required for snRNA gene expression. *Science* **318**, 1777–1779 (2007).
33. Baillat, D. *et al.* Integrator, a multiprotein mediator of small nuclear RNA processing, associates with the C-terminal repeat of RNA polymerase II. *Cell* **123**, 265–276 (2005).
34. Chapman, R.D. *et al.* Transcribing RNA polymerase II is phosphorylated at CTD residue serine-7. *Science* **318**, 1780–1782 (2007).
35. Stiller, J.W., McConaughy, B. & Hall, B. Evolutionary complementation for polymerase II CTD function. *Yeast* **16**, 57–64 (2000).
36. Egloff, S. & Murphy, S. Cracking the RNA polymerase II CTD code. *Trends Genet.* **24**, 280–288 (2008).
37. Jenuwain, T. & Allis, C. Translating the histone code. *Science* **293**, 1074–1080 (2001).
38. Gomes, N.P. *et al.* Gene-specific requirement for P-TEFb activity and RNA polymerase II phosphorylation within the p53 transcriptional program. *Genes Dev.* **20**, 601–612 (2006).
39. Medlin, J. *et al.* P-TEFb is not an essential elongation factor for the intronless human U2 snRNA and histone H2b genes. *EMBO J.* **24**, 4154–4165 (2005).
40. Kanin, E.I. *et al.* Chemical inhibition of the TFIIH-associated kinase Cdk7/Kin28 does not impair global mRNA synthesis. *Proc. Natl. Acad. Sci. USA* **104**, 5812–5817 (2007).
41. Lee, K.M. *et al.* Impairment of the TFIIH-associated CDK-activating kinase selectively affects cell cycle-regulated gene expression in fission yeast. *Mol. Biol. Cell* **16**, 2734–2745 (2005).
42. Serizawa, H., Conaway, J. & Conaway, R. Phosphorylation of C-terminal domain of RNA polymerase II is not required in basal transcription. *Nature* **363**, 371–374 (1993).
43. Akhtar, M.S. *et al.* TFIIH kinase places bivalent marks on the carboxy-terminal domain of RNA polymerase II. *Mol. Cell* **34**, 387–393 (2009).
44. Kim, M., Suh, H., Cho, E. & Buratowski, S. Phosphorylation of the yeast Rpb1 C-terminal domain at serines 2, 5, and 7. *J. Biol. Chem.* **284**, 26421–26426 (2009).
45. Glover-Cutter, K. *et al.* TFIIH-associated Cdk7 kinase functions in phosphorylation of C-terminal domain Ser7 residues, promoter-proximal pausing, and termination by RNA polymerase II. *Mol. Cell. Biol.* **29**, 5455–5464 (2009).
46. Patturajan, M., Conrad, N., Bregman, D. & Corden, J. Yeast carboxyl-terminal domain kinase I positively and negatively regulates RNA polymerase II carboxyl-terminal domain phosphorylation. *J. Biol. Chem.* **274**, 27823–27828 (1999).
47. Viladevall, L. *et al.* TFIIH and P-TEFb coordinate transcription with capping enzyme recruitment at specific genes in fission yeast. *Mol. Cell* **33**, 738–751 (2009).
48. Qiu, H., Hu, C. & Hinnebusch, A. Phosphorylation of the Pol II CTD by KIN28 enhances BUR1/BUR2 recruitment and Ser2 CTD phosphorylation near promoters. *Mol. Cell* **33**, 752–762 (2009).
49. Steinmetz, E.J. *et al.* Genome-wide distribution of yeast RNA polymerase II and its control by Sen1 helicase. *Mol. Cell* **24**, 735–746 (2006).
50. Neil, H. *et al.* Widespread bidirectional promoters are the major source of cryptic transcripts in yeast. *Nature* **457**, 1038–1042 (2009).
51. Xu, Z. *et al.* Bidirectional promoters generate pervasive transcription in yeast. *Nature* **457**, 1033–1037 (2009).
52. Holstege, F.C. & Young, R. Dissecting the regulatory circuitry of a eukaryotic genome. *Cell* **95**, 717–728 (1998).
53. Venters, B.J. & Pugh, B. A canonical promoter organization of the transcription machinery and its regulators in the *Saccharomyces* genome. *Genome Res.* **19**, 360–371 (2009).
54. Knight, Z.A. & Shokat, K.M. Features of selective kinase inhibitors. *Chem. Biol.* **12**, 621–637 (2005).
55. Ahn, S.H., Keogh, M. & Buratowski, S. Ctk1 promotes dissociation of basal transcription factors from elongating RNA polymerase II. *EMBO Open. EMBO J.* **28**, 205–212 (2009).
56. Arigo, J.T., Eyler, D., Carroll, K. & Corden, J. Termination of cryptic unstable transcripts is directed by yeast RNA-binding proteins Nrd1 and Nab3. *Mol. Cell* **23**, 841–851 (2006).
57. Thiebaut, M., Kisseleva-Romanova, E., Rougemaille, M., Boulay, J. & Libri, D. Transcription termination and nuclear degradation of cryptic unstable transcripts: a role for the nrd1-nab3 pathway in genome surveillance. *Mol. Cell* **23**, 853–864 (2006).
58. Kim, M. *et al.* Distinct pathways for snoRNA and mRNA termination. *Mol. Cell* **24**, 723–734 (2006).
59. Sheldon, K.E., Mauger, D. & Arndt, K. A requirement for the *Saccharomyces cerevisiae* Paf1 complex in snoRNA 3′ end formation. *Mol. Cell* **20**, 225–236 (2005).
60. Lee, W. *et al.* A high-resolution atlas of nucleosome occupancy in yeast. *Nat. Genet.* **39**, 1235–1244 (2007).

ONLINE METHODS

Genome-wide location and transcriptional analyses. ChIP with antibodies against Pol II (α RPB3) and the Ser7-P (4E12), Ser5-P (H14) and Ser2-P forms of Pol II was performed as described previously⁶¹ with several modifications (see **Supplementary Methods**). The ChIP samples were amplified using ligation-mediated PCR and hybridized to high density tiling microarrays from NimbleGen (Roche NimbleGen, Inc.). Total RNA samples were isolated before formaldehyde cross-linking during the ChIP experiments and were processed by Roche NimbleGen hybridization to high-density tiling microarrays having the same design as those used for the ChIP-chip experiments.

Data analysis. ChIP-chip immunoprecipitated data was mean-scaled against its respective 'input' sample data, and then the ratio of scaled immunoprecipitation to the input was \log_2 -transformed. For total RNA data, the probe intensities were divided by the peak intensity from the raw data histogram and then \log_2 -transformed. Both data types were subjected to computational repeat sequence masking based on probe-sequence repetitiveness relative to the sequence composition of the probes on the microarray (see **Supplementary Methods**). A moving average was used to smooth the microarray data, and baseline corrections were applied through comparison between polymerase and transcript data (see **Supplementary Methods**).

Average transcription unit analysis was applied to the data to obtain occupancy profiles normalized for gene length for every gene in gene sets I, II and III. This allowed for alignment of the occupancy patterns for all the genes in the genome (see **Supplementary Methods**). K-means clustering was performed to partition the genes into categories based on their occupancy profiles. These clusters were then manually collapsed into four representative groups. Clusters were refined through iterative silhouette score calculations, cluster reassignments and gene silhouette score filtering⁶² (see **Supplementary Methods**). Transcription factor enrichments were determined via hypergeometric probabilities calculated from published binding data⁶³.

Kinase assays. The kinase assay was performed as described previously⁶⁴. Briefly, 200 ng of GST-CTD₄ or GST-CTD₁₄ (four or fourteen repeats of YSPTSPS fused

to GST) or its alanine substitutions (2A, 5A and 7A) were phosphorylated by four different kinases or whole cell extract at 25 °C for one hour in a buffer containing 20 mM HEPES (pH 7.5), 2.5 mM EGTA, 15 mM magnesium acetate, 0.8 mM ATP, 10% (v/v) glycerol, protease inhibitors and phosphatase inhibitors (1 mM Na₃N, 1 mM NaF, 0.4 mM Na₃VO₃). We directly spotted 4 μ l from the reaction mix onto nitrocellulose membrane (GE Healthcare) and processed it further as a standard dot-blotting protocol. For the assay, a 1:50 (α Ser2-P), 1:500 (α Ser5-P) or 1:200 (α Ser7-P) dilution of primary rat IgG and 1:10,000 dilution of secondary HRP anti-rat IgG (Southern Biotech) antibodies were used.

For the Bur1as inhibition study, 200 ng of GST-CTD14 was used. TAP-tagged WT Bur1 and FLAG3 \times -tagged Bur1as were incubated with 5 μ M 3MB-PP1 for 5 min in kinase assay buffer without ATP at room temperature (20–24 °C). Following the inhibition, 0.8 mM ATP or 0.6 mM N6-benzyl-ATP was added, and the reaction was allowed to run for 30 min at room temperature. We directly spotted 5 μ l from the reaction mix onto nitrocellulose membrane and processed it as a standard dot-blotting protocol. For the assay, a 1:30 (α Ser2-P), 1:1,000 (α Ser5-P), or 1:100 (α Ser7-P) dilution of primary rat IgG and 1:12,500 dilution of secondary HRP anti-rat IgG (Southern Biotech) antibodies were used.

For ELISA, the recombinant kinase (100 ng) was incubated with excess CTD-peptide (YSPTSPSYSPTSPSYSPTSPSYSPTSPSC; Peptide Specialty Laboratories GmbH) linked to 96-well plates in a 25- μ l kinase buffer containing 20 mM Tris-Cl (pH 7.4), 20 mM NaCl, 10 mM MgCl₂, 1 μ M DTT and 2 μ M ATP at 28 °C for 60 min. Phosphorylation of CTD was quantitated via ELISA experiments after incubation with α Ser2-P-, α Ser5-P- and α Ser7-P-specific antibodies.

61. Kanin, E.I. *et al.* Chemical inhibition of the TFIIH-associated kinase Cdk7/Kin28 does not impair global mRNA synthesis. *Proc. Natl. Acad. Sci. USA* **104**, 5812–5817 (2007).
62. Rousseeuw, P. Silhouettes: a graphical aid to the interpretation and validation of cluster analysis. *J. Comput. Appl. Math.* **20**, 53–65 (1987).
63. Harbison, C.T. *et al.* Transcriptional regulatory code of a eukaryotic genome. *Nature* **431**, 99–104 (2004).
64. Ansari, A.Z., Ogirala, A. & Ptashne, M. Transcriptional activating regions target attached substrates to a cyclin-dependent kinase. *Proc. Natl. Acad. Sci. USA* **102**, 2346–2349 (2005).

Copyright of Nature Structural & Molecular Biology is the property of Nature Publishing Group and its content may not be copied or emailed to multiple sites or posted to a listserv without the copyright holder's express written permission. However, users may print, download, or email articles for individual use.